

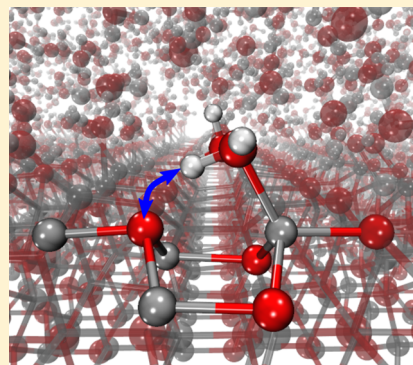
Solvent-Induced Proton Hopping at a Water–Oxide Interface

Gabriele Tocci and Angelos Michaelides*

Thomas Young Centre, London Centre for Nanotechnology and Department of Chemistry, University College London, London WC1E 6BT, United Kingdom

S Supporting Information

ABSTRACT: Despite widespread interest, a detailed understanding of the dynamics of proton transfer at interfaces is lacking. Here, we use ab initio molecular dynamics to unravel the connection between interfacial water structure and proton transfer for the widely studied and experimentally well-characterized water–ZnO(10 $\bar{1}$ 0) interface. We find that upon going from a single layer of adsorbed water to a liquid multilayer, changes in the structure are accompanied by a dramatic increase in the proton-transfer rate at the surface. We show how hydrogen bonding and rather specific hydrogen-bond fluctuations at the interface are responsible for the change in the structure and proton-transfer dynamics. The implications of this for the chemical reactivity and for the modeling of complex wet oxide interfaces in general are also discussed.

**SECTION:** Surfaces, Interfaces, Porous Materials, and Catalysis

Proton transfer in water is a process of central importance to a number of fields in science and technology. Consider, for example, proton conduction across polymeric membranes used in fuel cells¹ or through protein channels in cells.² Proton-transfer reactions are also key to many processes in catalysis such as the production of hydrogen from methanol or biomass^{3,4} or water formation.⁵ While it is notoriously difficult to characterize proton transfer under industrial or biological conditions, considerable insight and understanding has been gained by examining well-defined model systems. One such model system is the example of the solvated proton in pure liquid water.^{6–9} Another model system is water adsorbed on atomically flat solid surfaces. Indeed, whereas traditionally most work on well-defined water–solid interfaces has focused on structure characterization (e.g., ref 10 and references therein), increasingly the focus is turning to proton transfer and related properties such as surface acidity and water dissociation.^{11–17}

Of the various water–solid interfaces that have been examined, water on ZnO(10 $\bar{1}$ 0) plays a central role in heterogeneous catalysis^{4,18,19} and light harvesting.²⁰ It is also a well-defined system that has been the focus of a number of studies under ultra high vacuum (UHV) conditions,^{19,21} which have hinted at potentially interesting dynamical behavior. Specifically, Meyer et al. found that at monolayer (ML) coverage, one out of every two water molecules is dissociated, forming a so-called partially dissociated (PD) overlayer.¹⁹ Subsequently, they found that this PD overlayer could coexist with an overlayer of intact molecular (M) water.²¹ Moreover, they suggested that the two states may rapidly interchange such that an average configuration, intermediate between the two, is at times observed in their scanning tunneling microscopy images. These findings prompted a number of follow up

studies, which focused on the structure of water on the surface or on the level of dissociation.^{22–26} This previous work indicates that water on ZnO(10 $\bar{1}$ 0) might be a highly suitable system for investigating proton hopping in interfacial water. However, the key issue of how proton hopping occurs in this system and how it relates to the aqueous water environment is still not understood. Indeed, this is true for most water–solid interfaces, where major gaps in our understanding of the mechanisms of proton motion at interfaces remain.

This work focuses on understanding proton transfer at the liquid water–ZnO(10 $\bar{1}$ 0) interface. Although techniques for characterization of well-defined aqueous interfaces have emerged (e.g., refs. 11,12), probing the microscopic nature of proton transfer at interfaces remains a formidable challenge for experiment. On the other hand, ab initio molecular dynamics (AIMD), as we use here, has reached such a state of maturity that it is now possible to simulate bond-making and bond-breaking events at complex solid–liquid interfaces (see, e.g., refs 14, 15, 27, and 28). Here, we find that upon going from a water ML (characteristic of UHV) to a liquid film (LF) (characteristic of ambient conditions), changes in the structure and in the proton-transfer dynamics of interfacial water are observed. Although moderate alterations in the structure of the contact layer are found, the proton-transfer rate increases more than 10-fold. Analysis reveals that H-bond fluctuations induced by the liquid are responsible for the structural change and for the substantial increase in proton transfer. This effect is unlikely to be specific to water on ZnO, implying that proton transfer

Received: December 5, 2013

Accepted: January 15, 2014

Published: January 15, 2014

may be significantly faster under aqueous conditions than that at the low coverages typical of UHV-style studies. This fast proton transfer may also affect the chemical activity of a surface, being particularly relevant to heterogeneous catalysis under wet conditions.^{29–31}

The work reported here was carried out within the framework of density functional theory (DFT). Full details of the computational setup can be found in the Supporting Information.³² However, in brief, the key features of the simulations are that we used the PBE³³ exchange–correlation functional and the CP2K code.³⁴ The surface model is made of 6×3 primitive surface unit cells and a three-bilayer slab. There is one water molecule per primitive cell at ML coverage, whereas the LF is comprised of 144 molecules, resulting in a ~ 2 nm thick overlayer. The AIMD simulations are performed in the canonical ensemble close to room temperature. We performed extensive tests on the setup to explore the sensitivity of our results to issues such as basis set and exchange–correlation functional, including functionals that account for exact exchange and van der Waals forces.³² Overall, we find that, compared to other interfacial water systems, this one is rather benign, and none of our main conclusions are affected by the specific details of the DFT setup. In particular, although the importance of van der Waals dispersion forces between water molecules and water on surfaces is being increasingly recognized (see, e.g., refs 35–38), they do not have a significant impact on the dynamics of this system.³²

Let us first consider the adsorption of water on ZnO(10 $\bar{1}$ 0) at ML coverage. Figure 1a shows the spatial probability

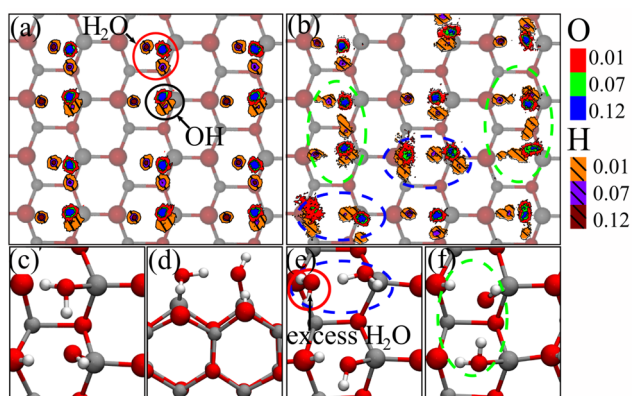


Figure 1. Spatial probability distribution function of the O and H atoms projected on ZnO(10 $\bar{1}$ 0) for (a) the water ML and (b) the contact layer of the LF. Gray, red, and white spheres are Zn, O, and H atoms, respectively. The topmost Zn and O surface atoms are shown using larger spheres. In (a), a H₂O and a OH that are connected via a H-bond are circled in red and black, respectively. (c) Top and (d) side views of the PD water dimer, which is the basic building block of the (2 × 1) overlayer structure. Snapshots of the LF showing water in a new type of structure enclosed in a blue oval (e) and the PD dimer structure enclosed in a green oval (f).

distribution function of the O and H atoms adsorbed on the surface at ML coverage. This illustrates the average structure of the overlayer projected onto the surface. Only the PD structure is observed, and it has a similar structure (bond lengths differ by <0.05 Å) to the zero temperature geometry-optimized structure. Figure 1c and d shows snapshots of the PD state in top and side views, respectively. The OHs and the H₂O sit in the trenches and are covalently bound to the surface Zn atoms.

A H-bond is formed between the surface Os and the H₂O and also between the surface OHs and the dissociated water. In addition, the H₂O donate a H-bond to the neighboring OHs and lie essentially flat on the surface, whereas the OHs are tilted up and point away from the surface.

A snapshot of the liquid water film is illustrated in Figure 2a, and in Figure 2b, the planar averaged density profile as a

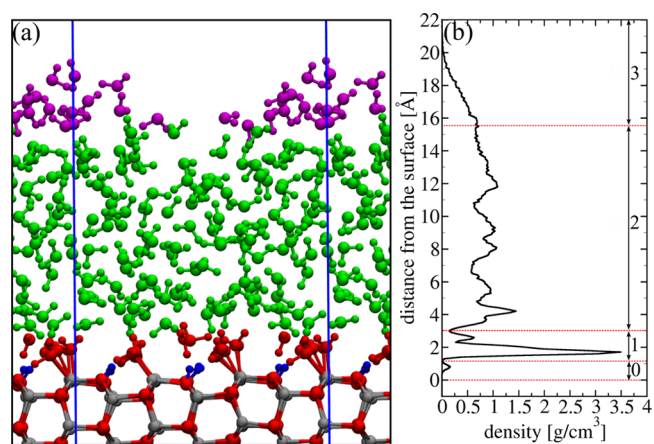


Figure 2. (a) Snapshot of a liquid water film on ZnO(10 $\bar{1}$ 0). (b) Planar averaged density profile as a function of the distance from the surface, where different regions are identified and labeled from 0 to 3. In (b), the zero in the distance is the average height of the top surface ZnO layer, and the density reported is the planar averaged density of adsorbed species. In (a), the top four surface layers are shown, and the water overlayer is colored according to the regions shown in the density profile (b). Regions (going from 0 to 3) correspond to chemisorbed H atoms, H₂O/OHs adsorbed on the surface, mainly bulk-like liquid water, and water in the liquid–vapor interface.

function of distance from the surface is reported. The density profile shows a pronounced layering, as previously reported for water on various substrates.^{17,39–42} For convenience, we discuss the density profile in terms of the regions observed and label them from 0 to 3. Region 0 shows up as a small peak close to the surface, and this corresponds to the chemisorbed Hs. These are the Hs that bond to the surface as a result of dissociation of some of the H₂O. The large peak of ~ 3.2 g/cm³ in region 1 at about 2.0 Å corresponds to a mixture of OHs and H₂O in immediate contact with the surface. The second peak in region 1 of about 0.7 g/cm³ also arises from a mixture of OHs and H₂O that sit on top of the surface O atom. Between regions 1 and 2, there is a depletion of H₂O; in region 2, the oscillations are damped until in region 3, the density decay, characteristic of the liquid–vacuum interface, is observed.⁴³

The structure of the contact layer in the LF differs from that in the ML in a number of ways (c.f. Figure 1a and b). First, although there are remnants of the (2 × 1) structure (see the green ovals in Figure 1b and f), the symmetry present at ML coverage is now broken. Second, the proton distribution is more delocalized in the contact layer of the LF than that in the ML. Third, and most notably, the coverage in the LF has increased to 1.16 ± 0.03 , with excess waters sitting in a new configuration on top of a surface O (circled in red in Figure 1e). At this new site, adsorption can happen either molecularly or dissociatively, and in either case, the adsorbate accepts a H-bond from a H₂O sitting on the top Zn site. Analysis of the overlayer reveals that H-bonding with the liquid above stabilizes the excess H₂O at the top O site, which gives rise to the higher

coverage.⁴⁴ Despite the structural change between the ML and the contact layer of the LF, we did not observe any exchange of water. Further, the level of dissociation is not altered in the two cases. This can be seen in Figure 3a and b, where the trajectory

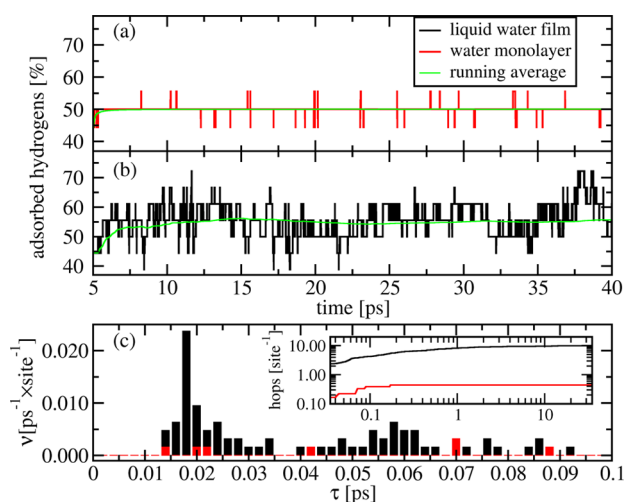


Figure 3. Time evolution of the percentage of H atoms adsorbed on the surface for (a) a water ML and (b) a liquid water overlayer. (c) Proton hopping frequency $\nu(\tau)$ as a function of the residence time τ for the LF (black) and the ML (red). The inset is a log–log plot of the total number of hops as a function of τ , obtained as $\int_0^\tau \nu(\tau') d\tau'$. The full 35 ps of analysis is shown in the inset.

of the percentage of adsorbed H atoms is reported for the two systems. At an average of 50% dissociation in the case of the ML and $55 \pm 5\%$ for the contact layer of the LF, the difference is not significant.⁴⁵

While the changes in the structure between the ML and LF are interesting and important, remarkable differences in the proton-transfer dynamics are observed. This is partly shown by the fluctuations in the percentage of adsorbed H atoms, which represent proton-transfer events to and from the surface (Figure 3). Clearly, by comparing Figure 3a and b, it can be seen that the fluctuations are much more pronounced in the LF than those in the ML. However, proton transfer to and from the surface is only part of the story as proton hopping between the H₂O and OHs is also observed in the contact layer of the LF. Indeed, this is already clear by looking at the proton distribution within the green ovals in Figure 1b. In the analysis reported in Figure 3c, all events are included, and the hopping of each proton is monitored. Specifically, we plot the hopping frequency ($\nu = \text{number of hops}/(\text{time} \times \text{sites})$) against τ . τ is defined as the time that a proton takes to return to the O to which it was initially bonded and therefore measures the lifetime of a proton hopping event, with larger values of τ corresponding to longer-lived events. Figure 3c thus reveals that proton transfer is more frequent in the LF than that in the ML. Specifically, in the LF, there are more events at all values of τ , with a maximum in the frequency distribution of about 0.02/(ps \times site) at $\tau \approx 20$ fs. In contrast, in the ML, the ν distribution never reaches values larger than 0.005/(ps \times site). The ~ 20 fs lifetime of the hopping events observed here is similar to the time scale of interconversion between Zundel-like and Eigen-like complexes in liquid water (<100 fs) obtained from femtosecond spectroscopy.⁴⁶ It is also in the same ballpark as other theoretical estimates of proton-transfer lifetimes obtained from work on proton transport in liquid

water or on other water–solid interfaces.^{9,47} The total number of hops (inset in Figure 3c) is $\sim 0.4/\text{site}$ in the ML but about 10/site in the LF. While only proton hopping between the overlayer and the surface is observed in the ML, in the LF, $\sim 1/4$ of the hops are within the contact layer, with the remaining 3/4 of all hops being to and from the surface. Proton hopping events are also longer-lived in the LF than those in the ML. This is demonstrated by the long tail in the frequency distribution of the LF and more clearly by the inset in Figure 3c, which shows that the longest hopping events are only about 0.2 ps in the ML but as long as ~ 4 ps in the LF. Events with a lifetime on the order of the picosecond are characteristic of Grotthus-like diffusion⁷ in liquid water or in other water–solid interfaces,^{15,17,47,48} which are however not observed here, although such a process may occur at longer time scales than we can simulate.²⁴

To gain further insight in the two systems, we plot in Figure 4 the free-energy surfaces (ΔF) for the various distinct proton-transfer events considered here. The free-energy surfaces have been obtained in a standard manner from $\Delta F = -k_B T \log P(\text{O} - \text{O}, \delta)$. The probability distribution $P(\text{O} - \text{O}, \delta)$ is a function of O–O distances and of δ , the position of the H with respect to the two Os. With reference to Figure 4, δ_{1-2} is defined as the difference in the distances between H and two oxygens, O₁ and O₂, that is, $\delta_{1-2} = (\text{O}_1 - \text{H}) - (\text{O}_2 - \text{H})$. Looking at Figure 4, we can see that there are some clear differences between the free-energy surfaces of the ML and those of the LF. First, the single minimum in Figure 4a shows that in the ML, protons do not hop between adsorbed H₂O and OHs. In contrast, in the LF, two clear minima are identified, revealing that hopping between adsorbed H₂O and OHs occurs readily. The approximate free-energy barrier of this process is ~ 100 meV. Second, proton hopping to and from the surface happens both in the ML (Figure 4b) and in the LF (Figure 4d), but the free-energy barrier is noticeably lower in the LF (~ 70 meV) than it is for the ML (~ 160 meV).

In order to understand why hopping increases so much upon going from ML to multilayer, we have examined the time dependence of the H-bonding network at the interface. This reveals an intimate connection between the local H-bonding environment of a molecule and its proclivity toward proton transfer. From the AIMD trajectory, we see this connection between the H-bonding environment and the hopping of individual protons, and we demonstrate in Figure 5a that this holds on average for the entirety of all water-to-surface proton hopping events. Specifically, Figure 5a shows the mean length of the O–H bonds that break in a proton-transfer event ($\langle \text{O}_w - \text{H} \rangle$) as a function of time. We find that this is correlated with $\langle \text{O}_w - \text{O}_d \rangle$, the mean distance between O_w and O_d, where O_d is the O of the nearest molecule donating a H-bond to O_w. At time $t < 0$, water is intact at a distance $\langle \text{O}_w - \text{H} \rangle \approx 1.0$ Å. Just before $t = 0$, the point at which the $\langle \text{O}_w - \text{H} \rangle$ bond breaks, there is a sharp increase in the $\langle \text{O}_w - \text{H} \rangle$ distance, and then, it levels off at ~ 1.4 Å, about 200 fs after dissociation. Accompanying these changes in the $\langle \text{O}_w - \text{H} \rangle$ distance are changes in $\langle \text{O}_w - \text{O}_d \rangle$ distances. Crucially, about 150 fs before proton transfer, there is a net decrease in the intermolecular separation $\langle \text{O}_w - \text{O}_d \rangle$ that shortens from about 3.1 to 2.9 Å. It can be seen clearly that this change in intermolecular separation occurs before the $\langle \text{O}_w - \text{H} \rangle$ bonds start to break, revealing that rearrangement in H-bonding is required prior to proton transfer. Similar behavior has recently been reported for the liquid water–InP(001) interface.¹⁷ Further, O–H bond lengthening due to the

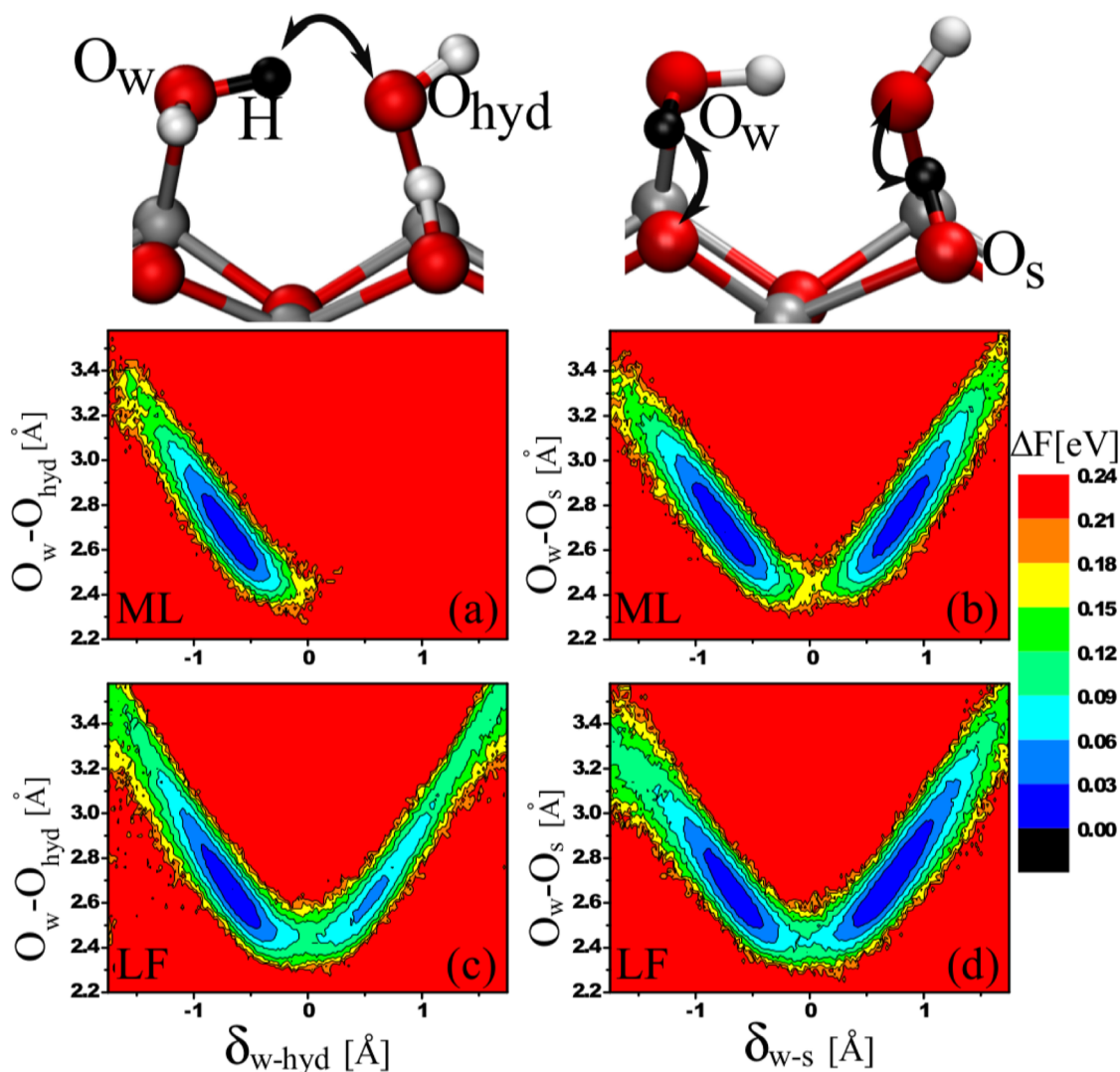


Figure 4. Free-energy, ΔF , contour plots for protons hopping between two Os as a function of the O–O distance and of the location of the protons between the two Os, δ . (a,b) Free energies for the protons hopping in the water ML simulation; (c,d) free energies in the LF simulation. As illustrated by the structures at the top of the figure, (a) and (c) refer to hopping between the Os in the contact layer, and (b) and (d) refer to hopping of protons to and from the surface. The contour lines and colors are shown on the same scales.

presence of additional water was reported for water on Al_2O_3 .¹⁶ Here, we illustrate that an increase in the O–H bond length occurs before the O–O distance decreases. Not only are the two distances correlated, but it is the decrease in the O–O distance that produces an increase in the O–H distance.

Through a careful series of additional calculations in which an individual proton-transfer event was examined, we established that the proton-transfer barrier depends critically on the intermolecular distance. As shown in Figure 5b, for relatively large distances of 3.4 Å, there is a small ~ 10 meV barrier. As the $\text{O}_w\text{--O}_d$ distance decreases, so too does the barrier until at ~ 3.1 Å where there is no barrier and the intact water state is not stable. Given that fluctuations in the H-bond distances are more pronounced in the LF than those in the ML and lead at times to relatively short $\text{O}_w\text{--O}_d$ separations, it is this that causes the more frequent proton transfer. An estimate of the H-bond distance fluctuations is obtained by computing the root-mean-square displacement of the O–O distances in the contact layer, which is 0.43 Å in the LF compared to the much smaller value of 0.15 Å in the ML. This increase is also the reason why hopping does not occur between neighboring

H_2O s and OHs in the ML while it does in the LF. H-bond distance fluctuations are also responsible for a proportion of events having a lifetime of ~ 1 ps or more (see the inset of Figure 3c), although actual hydrogen-bond forming and breaking may participate in this case. While we never observe H-bond forming or breaking in the ML, the H-bond lifetime is on the order of the picosecond in the LF, and this correlates well with the long-lived proton-transfer events.

We have shown that there are clear differences in the properties of water in contact with $\text{ZnO}(10\bar{1}0)$ upon going from UHV-like to more ambient-like conditions. Changes in the adsorption structure upon increasing the coverage above 1 ML have previously been predicted for a number of substrates including $\text{ZnO}(10\bar{1}0)$.^{11,16,24,51,52} The specific observation here is that the liquid water film leads to a $\sim 16\%$ increase in the water coverage and a breaking of the (2×1) periodicity observed at the ML. This arises because of H-bonding between the molecules in the contact layer and the molecules above it. It should be possible to verify this increased capacity for water adsorption using a technique such as in situ surface X-ray diffraction.

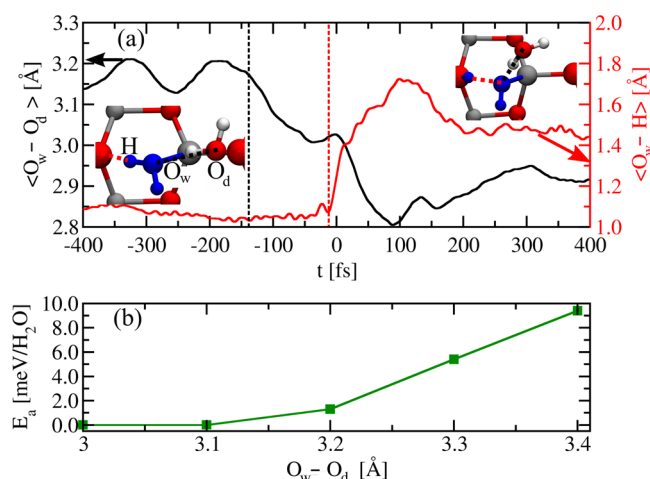


Figure 5. Analysis of the role of H-bond fluctuations on proton transfer. (a) Average O–O distance and average O–H distance as a function of time for all proton-transfer events to the surface. The O–O distance plotted (black line) is the distance between the O of the molecule involved in the proton-transfer event (O_w) and the O of the nearest molecule from which it accepts a H-bond (O_d). The O–H distance (red line) is the distance between O_w and the H that is involved in proton transfer. The black and red vertical lines indicate the approximate moment where there is a significant change in the $\langle O_w-O_d \rangle$ and $\langle O_w-H \rangle$ distances, respectively. The insets show snapshots of specific molecules before and after dissociation. (b) Activation energy (E_a) for water dissociation at ML coverage as a function of the O_w-O_d distance (calculated using VASP;^{49,50} see ref 32).

We have demonstrated that there is a substantial increase in the proton-transfer rate in the contact layer of the LF and that this is caused by H-bond fluctuations that lower the proton-transfer barrier. A H-bond-induced lowering of the dissociation barrier upon increasing the water coverage has been discussed before.^{11,16,19,48,53–55} Here, however, we have demonstrated that the barriers to dissociation and recombination are lowered in general because of the presence of the liquid. As in the case of liquid water and water on other substrates, we show (Figure 4) that there is a strong dependence between the proton-transfer barrier and the distance between the Os on either side of the hopping proton.^{6,7,15,56} However, we have also identified a connection between the molecule involved in the proton transfer and the molecules in its first solvation shell (Figure 5). This observation is somewhat similar to the structural diffusion of the excess proton in liquid water.^{7,8} The key difference between the two is that concerted H-bond breaking and making is required for proton diffusion in liquid water,⁷ while only fluctuations in the H-bond distance are needed for proton transfer (but not diffusion) to occur. Because fluctuations of the solvent provide the mechanism for the increased proton-transfer rate, a similar effect is expected also on other substrates, for example, on reactive metal surfaces upon which water dissociates.^{11,53}

Finally, because the barrier to proton transfer is sensitive to changes in specific H-bond distances, it is likely that implicit solvent models will be inadequate for this class of system as they do not account for H-bond fluctuations. A solvent-induced increase in the proton-transfer rate may also affect the chemical activity of the substrate and therefore have important consequences for heterogeneous catalysis under wet conditions.^{29–31,57} Given that the O–O distance correlates with

the barrier height and that H-bond distances of adsorbed H₂O/OHs are related to the lattice constant of the substrate, it might be possible to tailor the proton hopping rate through, for example, strain or doping of the substrate.

In conclusion, we have reported on a detailed AIMD study of water on ZnO. In so doing, we have tried to bridge the gap between studies of proton transfer in liquid water and low-coverage UHV-style work. This has revealed a substantial increase in the rate of proton transfer upon increasing the coverage from a ML to a liquid multilayer. We have tracked the enhanced proton-transfer rate to specific solvent-induced fluctuations in the H-bond network, which yield configurations with relatively short intermolecular distances wherein the barrier to proton transfer is lowered. These findings are potentially relevant to the modeling of wet interfaces in general and to heterogeneous catalysis.

■ ASSOCIATED CONTENT

Supporting Information

Further tests and computational details, including the computational setup, a comparison of the performance of difference exchange–correlation functionals for the calculation of water adsorption up to monolayer coverage, with the results of AIMD simulations of the LF using Grimme's dispersion correction, details of the calculations of the dissociation barriers at monolayer coverage, and a comparison with the results of previous theoretical studies on the level of water dissociation. This material is available free of charge via the Internet at <http://pubs.acs.org>.

■ AUTHOR INFORMATION

Corresponding Author

*E-mail: angelos.michaelides@ucl.ac.uk

Notes

The authors declare no competing financial interest.

■ ACKNOWLEDGMENTS

We are grateful for support from the FP7Marie Curie Actions of the European Commission, via the Initial Training Network SMALL (MCITN-238804). A.M. is supported by the European Research Council and the Royal Society through a Wolfson Research Merit Award. We are also grateful for computational resources to the London Centre for Nanotechnology and to the U.K.'s HPC Materials Chemistry Consortium, which is funded by EPSRC (EP/F067496), for access to HECToR.

■ REFERENCES

- (1) Steele, B. C. H.; Heinzel, A. Materials for Fuel-Cell Technologies. *Nature* **2001**, *414*, 345–352.
- (2) Garczarek, F.; Gerwert, K. Functional Waters in Intraprotein Proton Transfer Monitored by FTIR Difference Spectroscopy. *Nature* **2006**, *439*, 109–112.
- (3) Cortright, R. D.; Davda, R. R.; Dumesic, J. A. Hydrogen from Catalytic Reforming of Biomass-Derived Hydrocarbons in Liquid Water. *Nature* **2002**, *418*, 964–967.
- (4) Behrens, M.; Studt, F.; Kasatkin, I.; Kühl, S.; Hävecker, M.; Abild-Pedersen, F.; Zander, S.; Girgsdies, F.; Kurr, P.; Knief, B.-L.; et al. The Active Site of Methanol Synthesis over Cu/ZnO/Al₂O₃ Industrial Catalysts. *Science* **2012**, *336*, 893–897.
- (5) Michaelides, A.; Hu, P. Catalytic Water Formation on Platinum: A First-Principles Study. *J. Am. Chem. Soc.* **2001**, *123*, 4235–4242.
- (6) Tuckerman, M. E.; Marx, D.; Klein, M. L.; Parrinello, M. On the Quantum Nature of the Shared Proton in Hydrogen Bonds. *Science* **1997**, *275*, 817–820.

- (7) Marx, D. Proton Transfer 200 Years after von Grothuss: Insights from Ab Initio Simulations. *ChemPhysChem* **2006**, *7*, 1848–1870.
- (8) Marx, D.; Tuckerman, M. E.; Hutter, J.; Parrinello, M. The Nature of the Hydrated Excess Proton in Water. *Nature* **1999**, *397*, 601–604.
- (9) Berkelbach, T. C.; Lee, H.-S.; Tuckerman, M. E. Concerted Hydrogen-Bond Dynamics in the Transport Mechanism of the Hydrated Proton: A First-Principles Molecular Dynamics Study. *Phys. Rev. Lett.* **2009**, *103*, 238302.
- (10) Carrasco, J.; Hodgson, A.; Michaelides, A. A Molecular Perspective of Water at Metal Interfaces. *Nat. Mater.* **2012**, *11*, 667–674.
- (11) Andersson, K.; Ketteler, G.; Bluhm, H.; Yamamoto, S.; Ogasawara, H.; Pettersson, L. G. M.; Salmeron, M.; Nilsson, A. Autocatalytic Water Dissociation on Cu(110) at Near Ambient Conditions. *J. Am. Chem. Soc.* **2008**, *130*, 2793–2797.
- (12) Nagata, Y.; Pool, R. E.; Backus, E. H. G.; Bonn, M. Nuclear Quantum Effects Affect Bond Orientation of Water at the Water–Vapor Interface. *Phys. Rev. Lett.* **2012**, *109*, 226101.
- (13) Sulpizi, M.; Gaigeot, M. P.; Sprik, M. The Silica–Water Interface: How the Silanols Determine the Surface Acidity and Modulate the Water Properties. *J. Chem. Theory Comput.* **2012**, *8*, 1037–1047.
- (14) Cheng, J.; Sprik, M. Acidity of the Aqueous Rutile TiO₂(110) Surface from Density Functional Theory Based Molecular Dynamics. *J. Chem. Theory Comput.* **2010**, *6*, 880–889.
- (15) Wang, J.; Pedroza, L. S.; Poissier, A.; Fernandez-Serra, M. V. Photocatalytic Water Oxidation at the GaN(10 $\bar{1}$ 0) Water Interface. *J. Phys. Chem. C* **2012**, *116*, 14382–14389.
- (16) Hass, K. C.; Schneider, W. F.; Curioni, A.; Andreoni, W. The Chemistry of Water on Alumina Surfaces: Reaction Dynamics from First Principles. *Science* **1998**, *282*, 265–268.
- (17) Wood, B. C.; Scwegler, E.; Choi, W. I.; Ogitsu, T. Hydrogen-Bond Dynamics of Water at the Interface with InP/GaP (001) and the Implications for Photoelectrochemistry. *J. Am. Chem. Soc.* **2013**, *135*, 15774–15783.
- (18) Martínez-Suárez, L.; Frenzel, J.; Marx, D.; Meyer, B. Tuning the Reactivity of a Cu/ZnO Nanocatalyst via Gas Phase Pressure. *Phys. Rev. Lett.* **2013**, *110*, 086108.
- (19) Meyer, B.; Marx, D.; Dulub, O.; Diebold, U.; Kunat, M.; Langenberg, D.; Wöll, C. Partial Dissociation of Water Leads to Stable Superstructures on the Surface of Zinc Oxide. *Angew. Chem., Int. Ed.* **2004**, *48*, 6641–6645.
- (20) Law, M.; Greene, L. E.; Johnson, J. C.; Sayakally, R.; Yang, P. Nanowire Dye-Sensitized Solar Cells. *Nat. Mater.* **2005**, *4*, 455–459.
- (21) Dulub, O.; Meyer, B.; Diebold, U. Observation of the Dynamical Change in a Water Monolayer Adsorbed on a ZnO Surface. *Phys. Rev. Lett.* **2005**, *95*, 136101.
- (22) Wang, Y.; Muhler, M.; Wöll, C. Spectroscopic Evidence for the Partial Dissociation of H₂O on ZnO(10 $\bar{1}$ 0). *Phys. Chem. Chem. Phys.* **2006**, *8*, 1521.
- (23) Meyer, B.; Rabaa, H.; Marx, D. Water Adsorption on ZnO(10 $\bar{1}$ 0): from Single Molecules to Partially Dissociated Monolayers. *Phys. Chem. Chem. Phys.* **2006**, *8*, 1513–1520.
- (24) Raymand, D.; van Duin, A. C. T.; Goddard, W. A.; Hermansson, K.; Spangberg, D. Hydroxylation Structure and Proton Transfer Reactivity at the Zinc Oxide–Water Interface. *J. Phys. Chem. C* **2011**, *115*, 8573–8579.
- (25) Holthaus, S. g.; Köppen, S.; Frauenheim, T.; Colombi Ciacchi, L. Atomistic Simulations of the ZnO(1 $\bar{2}$ 10)/Water Interface: A Comparison between First-Principles, Tight-Binding, and Empirical Methods. *J. Chem. Theory Comput.* **2013**, *8*, 4517–4526.
- (26) Valtiner, M.; Todorova, M.; Grundmeier, G.; Neugebauer, J. Temperature Stabilized Surface Reconstructions at Polar ZnO(0001). *Phys. Rev. Lett.* **2009**, *103*, 065502.
- (27) Cicero, G.; Catellani, A.; Galli, G. Atomic Control of Water Interaction with Biocompatible Surfaces: The Case of SiC(001). *Phys. Rev. Lett.* **2004**, *93*, 016102.
- (28) Liu, L.-M.; Laio, A.; Michaelides, A. Initial Stages of Salt Dissolution Determined with Ab Initio Molecular Dynamics. *Phys. Chem. Chem. Phys.* **2011**, *13*, 13162.
- (29) Song, T.; Hu, P. Insight into the Solvent Effect: A Density Functional Theory Study of Cisplatin Hydrolysis. *J. Chem. Phys.* **2006**, *125*, 091101.
- (30) Haw, J.; Xu, T.; Nicholas, J. B.; Goguen, P. W. Solvent-Assisted Proton Transfer in Catalysis by Zeolite Solid Acids. *Nature* **1997**, *389*, 832–835.
- (31) Janik, M. J.; Davis, R. J.; Neurock, M. Anhydrous and Water-Assisted Proton Mobility in Phosphotungstic Acid. *J. Am. Chem. Soc.* **2005**, *127*, 5328–5245.
- (32) See the Supporting Information for further details on the computational setup (including tests on accuracy) and for a comparison with previous studies on the level of water dissociation.
- (33) Perdew, J. P.; Burke, K.; Ernzerhof, M. Generalized Gradient Approximation Made Simple. *Phys. Rev. Lett.* **1996**, *77*, 3865.
- (34) VandeVondele, J.; Krack, M.; Mohamed, F.; Parrinello, M.; Chassaing, T.; Hutter, J. QUICKSTEP: Fast and Accurate Density Functional Calculations Using a Mixed Gaussian and Plane Waves Approach. *Comput. Phys. Commun.* **2005**, *167*, 103.
- (35) Klimeš, J.; Michaelides, A. Perspective: Advances and Challenges in Treating van der Waals Dispersion Forces in Density Functional Theory. *J. Chem. Phys.* **2012**, *137*, 120901.
- (36) Santra, B.; Klimeš, J.; Alfè, D.; Slater, B.; Michaelides, A.; Car, R.; Scheffler, M. Hydrogen Bonds and van der Waals Forces in Ice at Ambient and High Pressures. *Phys. Rev. Lett.* **2011**, *107*, 185701.
- (37) Zhang, G.; Wu, J.; Galli, G.; Gygi, F. Structural and Vibrational Properties of Liquid Water from van der Waals Density Functionals. *J. Chem. Theory Comput.* **2011**, *7*, 3054–3061.
- (38) Carrasco, J.; Santra, B.; Klimeš, J.; Michaelides, A. To Wet or Not to Wet? Dispersion Forces Tip the Balance for Water-Ice on Metals. *Phys. Rev. Lett.* **2011**, *106*, 026101.
- (39) Liu, L.-M.; Krack, M.; Michaelides, A. Density Oscillations in a Nanoscale Water Film on Salt: Insight from Ab Initio Molecular Dynamics. *J. Am. Chem. Soc.* **2008**, *130*, 8572–8573.
- (40) Cicero, G.; Grossman, J. C.; Scwegler, E.; Gygi, F.; Galli, G. Water Confined in Nanotubes and between Graphene Sheets: A First Principle Study. *J. Am. Chem. Soc.* **2008**, *130*, 1871–1878.
- (41) Fenter, P.; Sturchio, N. C. Mineral–Water Interfacial Structures Revealed by Synchrotron X-ray Scattering. *Prog. Surf. Sci.* **2004**, *77*, 171.
- (42) Fukuma, T.; Ueda, Y.; Yoshioka, S.; Asakawa, H. Atomic-Scale Distribution of Water Molecules at the Mica–Water Interface Visualized by Three-Dimensional Scanning Force Microscopy. *Phys. Rev. Lett.* **2010**, *104*, 016101.
- (43) Kuo, I. F. W.; Mundy, C. J. An Ab Initio Molecular Dynamics Study of the Aqueous Liquid–Vapor Interface. *Science* **2004**, *303*, 658–660.
- (44) From a separate set of geometry optimizations, we established that the contact layer of the LF (without the liquid overlayer above it) is 90 ± 30 meV/H₂O less stable than the structure of the ML. This value was obtained by comparing the energy of the optimized ML with the average energy of five characteristic snapshots of the contact layer from the LF simulation (each relaxed in the absence of the liquid overlayer).
- (45) Raymand et al. predicted an increase to 80% dissociation in a reactive force field based study.²⁴ See ref 32 for a discussion on this difference.
- (46) Woutersen, S.; Bakker, H. J. Ultrafast Vibrational and Structural Dynamics of the Proton in Liquid Water. *Phys. Rev. Lett.* **2006**, *96*, 138305.
- (47) Akimov, A. V.; Muckerman, J. T.; Prezhdo, O. V. Nonadiabatic Dynamics of Positive Charge during Photocatalytic Water Splitting on GaN(10 $\bar{1}$ 0) Surface: Charge Localization Governs Splitting Efficiency. *J. Am. Chem. Soc.* **2013**, *135*, 8682–8691.
- (48) Wood, B. C.; Scwegler, E.; Choi, W. I.; Ogitsu, T. Surface Chemistry of GaP (001) and InP (001) in Contact with Water. *J. Phys. Chem. C* **2014**, *118*, 1062–1070.

(49) Kresse, G.; Hafner, J. *Ab Initio* Molecular Dynamics for Liquid Metals. *Phys. Rev. B* **1993**, *47*, 558–561.

(50) Kresse, G.; Furthmüller, J. Efficient Iterative Schemes for *Ab Initio* Total-Energy Calculations Using a Plane-Wave Basis Set. *Phys. Rev. B* **1996**, *54*, 11169–11186.

(51) Liu, L.-M.; Zhang, C.; Thornton, G.; Michaelides, A. Structure and Dynamics of Liquid Water on Rutile $\text{TiO}_2(110)$. *Phys. Rev. B* **2010**, *82*, 161415(R).

(52) Liu, L.-M.; Zhang, C.; Thornton, G.; Michaelides, A. Reply to “Comment on ‘Structure and Dynamics of Liquid Water on Rutile $\text{TiO}_2(110)$ ’”. *Phys. Rev. B* **2012**, *85*, 167402.

(53) Michaelides, A.; Alavi, A.; King, D. A. Different Surface Chemistries of Water on $\text{Ru}\{0001\}$: From Monomer Adsorption to Partially Dissociated Bilayers. *J. Am. Chem. Soc.* **2003**, *125*, 2746–2755.

(54) Odellius, M. Mixed Molecular and Dissociative Water Adsorption on $\text{MgO}[100]$. *Phys. Rev. Lett.* **1999**, *82*, 3919–3922.

(55) Hu, X. L.; Klimeš, J.; Michaelides, A. Proton Transfer in Adsorbed Water Dimers. *Phys. Chem. Chem. Phys.* **2010**, *12*, 3953–3956.

(56) Li, X. Z.; Probert, M. I. J.; Alavi, A.; Michaelides, A. Quantum Nature of the Proton in Water–Hydroxyl Overlayers on Metal Surfaces. *Phys. Rev. Lett.* **2010**, *104*, 066102.

(57) Merte, L. R.; Peng, G.; Bechstein, R.; Rieboldt, F.; Farberow, C. A.; Grabow, L. C.; Kudernatsch, W.; Wendt, S.; Lægsgaard, E.; Mavrikakis, M.; et al. Water-Mediated Proton Hopping on an Iron Oxide Surface. *Science* **2012**, *336*, 889–893.